ACS Synthetic Biology
Cite This: ACS Synth. Biol. XXXX, XXX, XXX−XXX
Letter
pubs.acs.org/synthbio

De Novo Synthesis of Basal Bacterial Cell Division Proteins FtsZ, FtsA, and ZipA Inside Giant Vesicles

Takumi Furusato,[†,§] Fumihiro Horie,[†,§] Hideaki T. Matsubayashi,[†,∥,§] Kazuaki Amikura,[†] Yutetsu Kuruma,[‡] and Takuya Ueda*[,†]

[†]Department of Computational Biology and Medical Sciences, Graduate School of Frontier Sciences, The University of Tokyo, Bldg. FSB-401, 5-1-5 Kashiwanoha, Kashiwa, Chiba 277-8562, Japan

[‡]Earth-Life Science Institute, Tokyo Institute of Technology, 2-12-1-IE-1, Ookayama, Meguro-ku, Tokyo, 152-8550, Japan

Supporting Information

ABSTRACT: Cell division is the most dynamic event in the cell cycle. Recently, efforts have been made to reconstruct it using the individual component proteins to obtain a better understanding of the process of self-reproduction of cells. However, such reconstruction studies are frequently hampered by difficulties in preparing membrane-associated proteins. Here we demonstrate a *de novo* synthesis approach based on a cell-free translation system. Genes for fundamental cell division proteins, FtsZ, FtsA, and ZipA, were expressed inside the lipid compartment of giant vesicles (GVs). The synthesized proteins showed polymerization, membrane localization, and eventually membrane deformation. Notably, we found that this morphological change of the vesicle is forced by only FtsZ and ZipA, which form clusters on the membrane at the vesicle interior. Our cell-free approach provides a platform for studying protein dynamics associated with lipid membrane and paves the way to create a synthetic cell that undergoes self-reproduction.

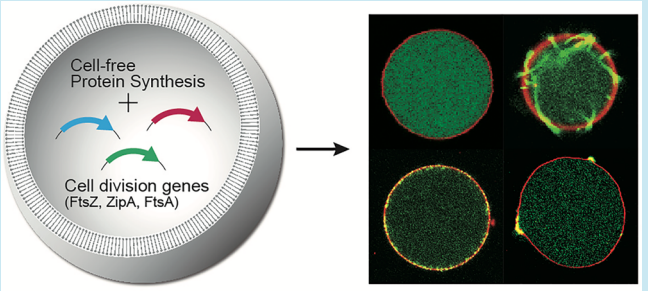

KEYWORDS: *cell-free translation, PURE system, cell division, FtsZ, giant vesicles, synthetic cell*

Bacterial cytokinesis is driven by protein machinery known as the divisome.[1,2] This machinery is composed of proteins found in the cytosol, cytoplasmic membrane, and cell wall. This protein network spatiotemporally orchestrates the dynamic cell division process. In most bacteria, divisome assembly is initiated by formation of the Z-ring, a contractile ring that is based on the polymer structure of the tubulin homologue protein FtsZ. While FtsZ itself does not have any membrane targeting motifs, it is anchored to the cytoplasmic membrane by interactions with FtsA and/or ZipA. FtsA binds to the membrane *via* its C-terminal amphipathic helix,[3] whereas ZipA is integrated into the membrane by its N-terminal single-transmembrane helix.[4] These three subunits constitute the backbone of the Z-ring and lead to the subsequent division processes. Thus, it is important to understand how these key proteins achieve membrane interaction and generate the constrictive force of the Z-ring on the cytoplasmic membrane.

To elucidate the molecular mechanism of the three subunits, biochemical and biophysical research is crucial. However, it has been notoriously difficult to purify *E. coli* FtsA in its native form.[5] Largely due to this problem, *in vitro* studies have been hampered, and some biochemical properties, such as lipid dependence of membrane binding and the role of nucleotide binding, remain to be elucidated. As for ZipA, despite the biological importance of its N-terminal transmembrane domain,[6,7] it is frequently replaced with a His-tag that artificially interacts with Ni-chelating lipids.[8,9] This is a workaround employed by previous studies due to the troublesome purification process of full-length ZipA.[10,11] Moreover, although great progress has been made with reconstructing the initial steps of cell division with supported lipid layer[8,11] and liposome,[9,12−14] some technical challenges still remain unresolved. For instance, supported lipid layer is too rigid to address the mechanical properties of cell division. Meanwhile, the liposome approach has difficulty in reconstructing membrane proteins with correct topology due to the use of detergents during protein purification. Furthermore, simple reactions of recombinant proteins do not faithfully reflect the periodic nature of the cell cycle.

De novo cell-free synthesis is one of the most promising methods to overcome these technical difficulties. Bypassing troublesome protein purification processes, cell-free synthesis achieves simple and rapid protein preparation. Cotranslational membrane integration enables us to reconstruct transmembrane proteins directly without using detergents and in a topologically biased manner.[15,16] Accumulating literature has also shown the compatibility of cell-free synthesis systems with various lipid vesicle preparation methods.[17−20] Furthermore, *de*

Received: October 4, 2017
Published: March 7, 2018

DOI: 10.1021/acssynbio.7b00350
ACS Synth. Biol. XXXX, XXX, XXX−XXX

novo synthesis can accurately reflect all events from gene expression to protein dynamics that take place in living cells.

In this study, we used a reconstructed cell-free protein synthesis system, PURE system,[21] for the reconstruction of bacterial initial cell division proteins FtsZ, FtsA, and ZipA (Figure 1A). The advantage of using the PURE system is that endogenous cell division proteins and unknown factors derived from host bacteria can be eliminated from the reaction mixture. The proteins were successfully synthesized at the micromolar level in a batch and those functions were verified by biochemical assays. Furthermore, the technique was also applied in giant vesicles (GVs) and the *de novo* synthesized proteins showed some molecular assembly leading to membrane deformation. Our method based on the PURE system and GVs provides a rational strategy to study the dynamics of multicomponent protein machinery on the lipid bilayer in a purified system and also to develop a minimal self-reproducible system by a bottom-up approach.

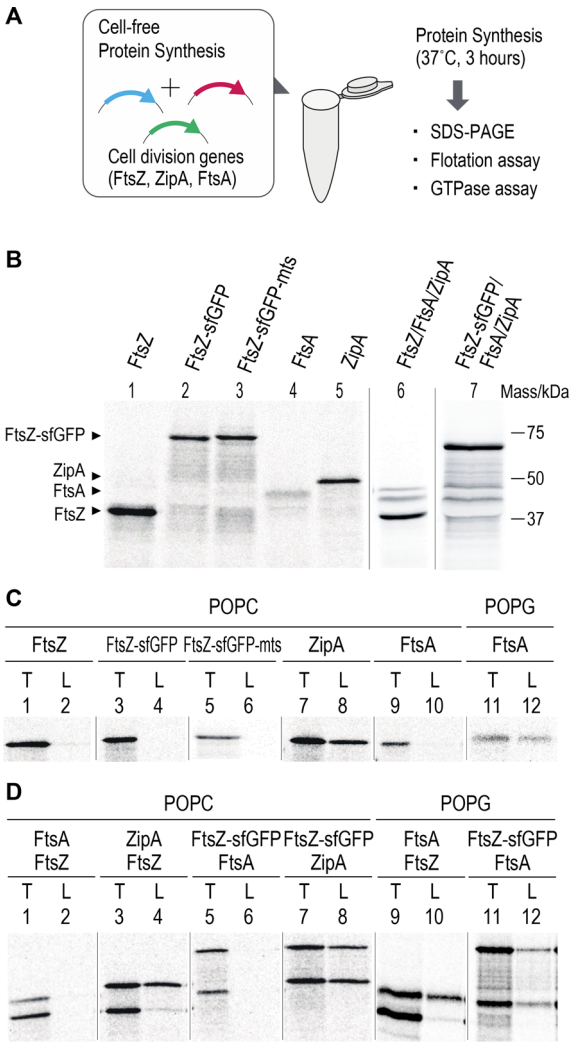

Figure 1. *In vitro* expression of cell division proteins. (A) Schematic representation of cell-free synthesis and following biochemical assays. (B) Protein syntheses by single or multiple gene expression. Positions of proteins and molecular mass are indicated beside the gel. (C,D) Flotation assay to assess membrane binding activity of the synthesized proteins. "T" and "L" represent total fraction and liposome fraction, respectively (see Methods). Liposomes were made of 99.5 mol % POPC/0.5 mol % Rhod-DOPE (POPC) or 95 mol % POPG/5 mol % Rhod-DOPE (POPG). Proteins were synthesized in single (C) or multiple (D) expression conditions. The order of protein labels in (D) corresponds to the order of protein bands in the gel. (B–D) The synthesized proteins were visualized and quantified by ^{35}S-methionine.

FtsZ polymerization and other higher-order structures have been reported to require 0.7 μM and 2 μM monomer proteins, respectively, in the presence of 10 mM Mg^{2+} ions.[22] To achieve this, we used PURE*frex* 2.0 (GeneFrontier Corporation), the latest version possessing the highest expression level among the PURE system series. For quantification under batch condition, the synthesized proteins were cotranslationally labeled with ^{35}S-methionine and distinguished from intrinsic proteins in PURE system such as translational factors. In single gene expression, we successfully expressed FtsZ (5.9 ± 0.2 μM), C-terminal superfolder GFP (sfGFP) fusion of FtsZ (FtsZ-sfGFP, 2.7 ± 0.3 μM), FtsZ-sfGFP fused with MinD membrane targeting sequence (mts) (FtsZ-sfGFP-mts, 1.5 ± 1.0 μM), FtsA (1.4 ± 0.7 μM), and ZipA (4.0 ± 0.8 μM) (Figure 1B, Lanes 1–5). Simultaneous expression of multiple genes was also available (Figure 1B, Lanes 6 and 7, Figure 1D). When the proportion of introduced DNA was adjusted to 2.0 nM FtsZ:3.0 nM FtsA:0.2 nM ZipA, the stoichiometry of the synthesized proteins was 2.2 μM FtsZ:1.4 μM FtsA:0.4 μM ZipA. Meanwhile, 1.5 μM FtsZ-sfGFP, 0.7 μM FtsA, and 1.2 μM ZipA were synthesized at the same DNA proportions.

In consistent with solubility database of *E. coli* proteins synthesized in the classical PURE system,[23] solubility assay based on centrifugation of the protein synthesis mixture revealed that almost 70% of synthesized FtsZ, FtsA, and ZipA maintained a soluble state, suggesting that they folded correctly even in the absence of any chaperone proteins and membrane (Figure S1, Supporting Information). The solubility of sfGFP fused FtsZ, FtsA and ZipA was also higher than 70%, except for sfGFP-ZipA (61%) (Figure S1, Supporting Information). Specific GTPase activity was detected depending on the synthesis of FtsZ; this was further supported by the loss of activity in the FtsZ3 (T108A) mutant, which loses GTP binding and hydrolysis activity[24] (Figure S2, Supporting Information). The measured GTP hydrolysis rates of FtsZ and FtsZ-sfGFP were 0.74 ± 0.17 and 2.34 ± 0.63 nmol Pi release/nmol FtsZ/min, respectively, which are in the same range as previously reported.[24] This result indicates that the synthesized proteins maintain enzymatic activity. Moreover, since GTPase activity depends on FtsZ polymerization, data also suggested that cell-free synthesized FtsZ is capable of assembling into FtsZ protofilaments. Of note, specific activity of FtsZ-sfGFP was three times higher than that of FtsZ alone, even though the synthesized protein concentration of FtsZ-sfGFP was roughly half that of FtsZ and less favorable for polymerization-dependent GTPase reaction. This implies that C-terminal sfGFP fusion facilitated the polymerization of FtsZ or directly enhanced GTPase activity. This finding may also account for why FtsZ-GFP cannot fully complement the thermosensitive FtsZ mutation in *E. coli*.[25]

To evaluate the function of synthesized proteins further, we next assessed the ability of membrane binding by using a flotation assay with small lipid vesicles.[26] In this assay, proteins were synthesized in the outside of vesicles. Membrane-bound proteins were collected with floated vesicles in an upper layer of a sucrose gradient (liposome fraction: L) and compared to the input (total fraction: T) (Figure S3A, Supporting Information). As expected, FtsZ and FtsZ-sfGFP did not show membrane binding in a single protein expression condition (Figure 1C,

DOI: 10.1021/acssynbio.7b00350
ACS Synth. Biol. XXXX, XXX, XXX−XXX

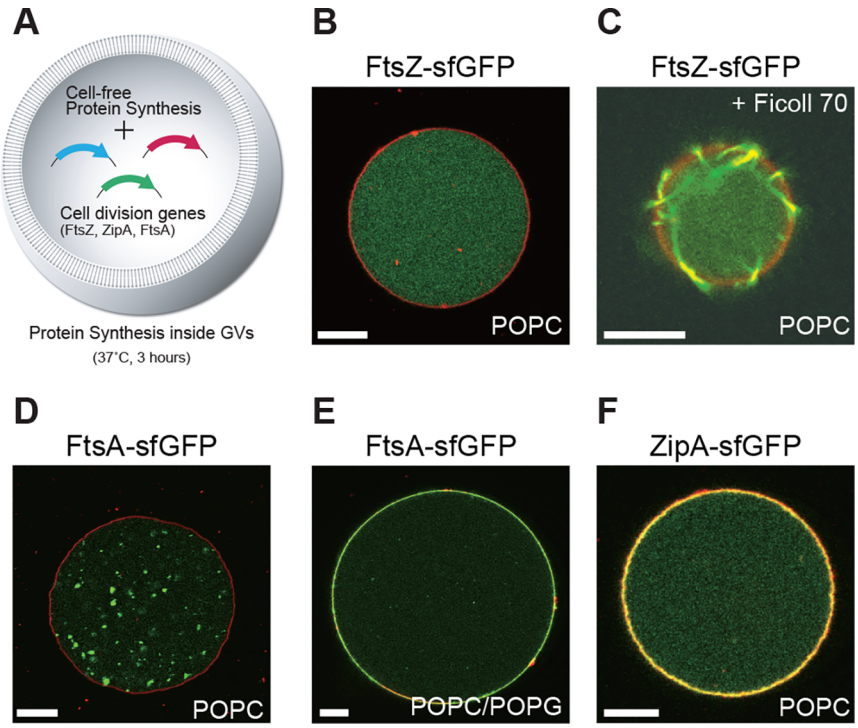

Figure 2. Single protein expression in GVs. (A) Schematic representation of protein expression in GVs. (B−F) Confocal microscope images of GVs. Green fluorescence and red fluorescence represent sfGFP and Rhod-DOPE, respectively. The expressed proteins are indicated above the images. POPC denotes 100% POPC GV, while POPC/POPG represents 80% POPC/20% POPG GV (see Methods). In the "+ Ficoll 70" condition, 12% (w/v) Ficoll 70 was added to the inside of GVs. Scale bars indicate 10 μm.

Lanes 1−4). We also tested FtsZ-sfGFP-mts; however, we did not observe membrane binding of FtsZ-sfGFP-mts to POPC liposomes in our flotation assay (Figure 1C, Lanes 5 and 6). Considering that monomeric MinD mts did not bind to zwitterionic lipids[27] and membrane binding of FtsZ-YFP-mts to 100% of PC liposomes depended on FtsZ polymerization by GTP addition,[28] the lack of POPC binding of FtsZ-sfGFP-mts was probably because FtsZ-sfGFP-mts monomer concentration was shifted to below the polymerization threshold after a dilution step in the flotation assay procedure. In great contrast, a large part of ZipA was collected from the membrane fraction, indicating strong interaction by the N-terminal transmembrane helix (Figure 1C, Lanes 7 and 8). FtsA showed binding to anionic POPG liposomes, but did not to zwitterionic POPC liposomes (Figure 1C, Lanes 9−12, Figure S3B, Supporting Information). This was in agreement with previous studies showing that MinD mts requires anionic lipids to fold amphipathic helices[27] and FtsA mts has a helix with a similar amino acid pattern.[3]

To confirm whether the cell-free synthesized FtsA and ZipA are functional as membrane tethers for FtsZ, we performed flotation assay under coexpression condition. In contrast to FtsZ-sfGFP single expression, coexpression of ZipA brought considerable amounts of FtsZ-sfGFP to the membrane fraction (Figure 1D, Lanes 7 and 8). Similar recruitment was also seen in FtsA, but, consistent with the result for FtsA alone, it depended on anionic POPG lipid (Figure 1D, Lanes 5, 6, 11, and 12). Such membrane recruitment by anchor proteins was slightly detectable for FtsZ without sfGFP fusion (Figure 1D, Lanes 3, 4, 9, and 10). However, membrane binding of FtsZ was less than that of FtsZ-sfGFP. Considering the results of GTPase assay, this higher affinity is likely because of the higher polymerization activity of FtsZ-sfGFP, which leads to FtsZ-sfGFP polymer elongation and increases interaction sites for anchor proteins. Another explanation is that the gene fusion of bulky and tightly folded sfGFP protein to the C-terminus end influenced the conformation of the C-terminal peptide of FtsZ, the binding site for ZipA and FtsA, and enhanced the interaction of FtsZ monomer with anchor proteins. Because no recruitment was observed for sfGFP (Figure S3C, Supporting Information), this membrane tethering was undoubtedly specific to FtsZ and the difference between FtsZ and FtsZ-sfGFP was not due to the unspecific interaction of sfGFP with anchor proteins. Therefore, our data suggest that cell-free synthesized ZipA and FtsA are capable of binding membrane and recruiting FtsZ.

Next, we performed protein expression inside GVs (Figure 2A). In the process of GV preparation, 200 mM sucrose was added inside the vesicles with the reaction mixture of PURE*frex* 2.0 buffer in order to balance osmolality with the external buffer containing 200 mM glucose. Because the previous report showed that the GVs encapsulation of the PURE system by emulsion transfer method does not significantly change the yield and stoichiometry of protein expression compared to the batch condition,[29] we supposed the protein expression condition of inside GVs are comparable to that of batch mode except for sucrose. Expression level of FtsZ and FtsZ-sfGFP in the presence of 200 mM sucrose was tested in batch mode and showed 26 ± 4% increase for FtsZ and 18 ± 7% decrease for FtsZ-sfGFP (p-values of student's t-test are <0.0031 (FtsZ) and <0.051 (FtsZ-sfGFP), Figure S4, Supporting Information). Although the effect of sucrose addition on protein synthesis is not negligible, the total expression level was expected to be still high enough for FtsZ polymerization. For the GV experiment, first, we observed the localization patterns of each protein upon single expression.

DOI: 10.1021/acssynbio.7b00350
ACS Synth. Biol. XXXX, XXX, XXX−XXX

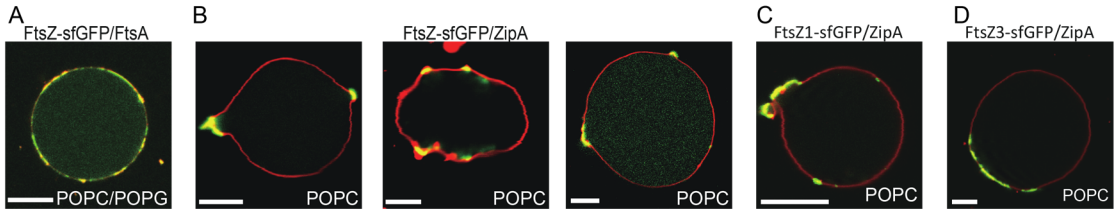

Figure 3. Multisubunit coexpression in GVs. (A–D) Confocal microscope images of GVs. Color representation and description of proteins and lipid condition are same as described in Figure 2. Input DNA concentration of each conditions are 5 nM FtsZ-sfGFP/10 nM FtsA (A), 5 or 6 nM FtsZ-sfGFP/3.8 nM ZipA (B), 6 nM FtsZ1(A70T)-sfGFP/6 nM ZipA (C), 6 nM FtsZ3(T108A)-sfGFP/6 nM ZipA (D). Scale bars indicate 10 μm.

Protein localization was visualized by the fluorescence of sfGFP. FtsZ-sfGFP showed dispersed fluorescence in the vesicle lumen, as was the case for single expression of sfGFP alone, but some punctate fluorescence was uniquely observed in FtsZ-sfGFP (Figure 2B, S5A and S11A, Supporting Information), possibly indicating that some FtsZ-sfGFP units assembled into small structures detectable by fluorescence microscopy. However, bundle formation or other higher-order structures were not observed in this condition. To imitate the intracellular crowded environment, we added Ficoll 70 at 12% (w/v), exceeding the reported threshold for FtsZ bundling.[30,31] Ficoll 70 addition had no significant additional effect on protein synthesis in batch mode compared to 200 mM sucrose condition (p-values of student's t-test are >0.17 (FtsZ) and >0.67 (FtsZ-sfGFP), Figure S4, Supporting Information). Under this condition, FtsZ-sfGFP fluorescence exhibited bundle-like structures in the periphery of the lipid membrane (Figure 2C, Figure S11B, Supporting Information), indicating that the effective concentration of FtsZ-sfGFP was increased above the threshold by adding Ficoll. 3D reconstruction of z-stack images revealed mesh structures of FtsZ bundles spreading on the inner surface of GV membrane (Figure S6, Supporting Information). This result clearly show that the cell-free synthesized FtsZ is able to assemble into protofilaments and bundles. Interestingly, however, the localization pattern of FtsZ bundles was slightly different from previously reported results, in which bundles were also observed in vesicle lumen.[31]

Single expression of sfGFP-FtsA or FtsA-sfGFP in POPC-based GVs also showed a luminal distribution and more apparent punctate structures (Figure 2D, Figure S5B and S11C, Supporting Information). Although it is unclear how these puncta are formed, solubility assay revealed that sfGFP tagged FtsA has similar solubility to that of FtsA alone, indicating that these puncta are not unfolded protein aggregates (Figure S1, Supporting Information). In the presence of 20% POPG lipids, which is the physiological level, both N and C terminal sfGFP-fused FtsA showed clear membrane localization in many GVs (Figure 2E, Figure S5C, S11D and S11E, Supporting Information). The membrane localization was more evident in line scan plot of sfGFP intensity (Figure S8, Supporting Information). This localization pattern was identical to the previous results of *Streptococcus pneumoniae* FtsA inside GVs containing 40% egg PC, 10% DMPC, 25% PG, and 25% cardiolipin.[14] In our condition, the percentage of GVs showing FtsA membrane localization was 42% (5 out of 12) in the case of N-terminal sfGFP fusion and 80% (4 out of 5) in that of C-terminal fusion, respectively. Consistent with our flotation assay, these data further supported the anionic lipid dependence of FtsA membrane binding. Since the inner leaflet of the cytoplasmic membrane is negatively charged by acidic phospholipids, similar localization of FtsA is thought to occur within the cell.

When ZipA-sfGFP was expressed in POPC GVs, it localized at the membrane in all the observed GVs (33 out of 33, Figure 2F, Figure S8 and S11F, Supporting Information). This membrane localization was lost in the case of N-terminal sfGFP fusion, sfGFP-ZipA, most likely because the fusion of a bulky sfGFP protein disturbed the membrane insertion of N-terminal ZipA transmembrane helix (Figure S5D, Supporting Information). Supporting the flotation assay results, the data indicated that ZipA can be integrated into the lipid bilayer by N-terminus transmembrane helix, unless the helix is masked by a bulky soluble protein. On the other hand, in the presence of 20% POPG, the membrane localization of ZipA-sfGFP was slightly reduced and, instead, heterogeneous patterns appeared in the vesicle lumen, suggesting anionic lipids inhibit the membrane integration of ZipA (Figure S5E and S8E, Supporting Information). Consistent with this result, our flotation assay data indicates that membrane association of ZipA with POPG liposome is relatively less than that with POPC liposome (Figure S3D, Supporting Information).

To visualize protein interactions by microscopic observation, we next performed coexpression of multiple components in GVs. First, we coexpressed FtsZ-sfGFP and FtsA in 20% POPG GVs. When the proteins were synthesized at a DNA ratio of 1 nM FtsZ-sfGFP to 10 nM FtsA, clear membrane localization of FtsZ-sfGFP fluorescence was observed (Figure S7A, Supporting Information). Because neither sfGFP nor FtsZ-sfGFP has affinity to 20% POPG membrane (Figure S5G and S5H, Supporting Information), the data showed that FtsZ was specifically recruited to the membrane by the synthesized FtsA. At a lower ratio of FtsZ-sfGFP to FtsA (0.2 nM FtsZ-sfGFP to 10 nM FtsA), the membrane localization was weakened and FtsZ-sfGFP distributed more in vesicle lumen (Figure S7B, Supporting Information), likely because FtsZ-sfGFP concentration fell below the threshold for FtsZ polymerization and the membrane recruitment of FtsZ by FtsA, which depends on FtsZ polymerization,[8] was largely lost. Conversely, when FtsZ-sfGFP concentration is relatively higher at the DNA ratio of 5 nM FtsZ-sfGFP to 10 nM FtsA, FtsZ-sfGFP fluorescence formed clusters on the GV membrane (Figure 3A and S12C). This membrane recruitment of FtsZ by FtsA was found in 47% of observed GVs (15 out of 32). Taken together, coexpression data clearly shows the synthesized FtsA is functional to tether FtsZ, likely FtsZ polymers, to the lipid membrane. It is also noteworthy that functional FtsA protein, which has the identical amino acid sequence to wild-type *E. coli* protein, can be prepared in a few hours without any troublesome purifications.

Next, we coexpressed FtsZ-sfGFP and ZipA in POPC 100% GVs. First, the proteins were synthesized at a DNA ratio of 6

DOI: 10.1021/acssynbio.7b00350
ACS Synth. Biol. XXXX, XXX, XXX–XXX

nM FtsZ-sfGFP to 11 nM ZipA. In contrast to the luminal localization of FtsZ-sfGFP alone, coexpression of ZipA partially recruited FtsZ-sfGFP to the membrane (Figure S7C, Supporting Information). In agreement with flotation assay data, this result indicates that synthesized ZipA functions as a membrane anchor for FtsZ. Fluorescence of the membrane-targeted FtsZ-sfGFP was not distributed homogeneously, but formed clustered regions on the membrane. This was different from previously reported results, in which FtsZ was recruited by His-tagged ZipA anchored by Ni-NTA lipid and distributed more globally on the membrane.[9] Considering that ZipA forms a homodimer through the interaction between two transmembrane helices and bridges FtsZ filaments,[7] our data strongly suggest that ZipA transmembrane helix has a role in FtsZ-ZipA complex clustering. When the input DNA ratio of FtsZ-sfGFP to ZipA was balanced around 1:1, membrane localization of FtsZ-sfGFP became clearer (Figure 3B and S12B, Supporting Information). In this condition, 77% (17 out of 22) showed membrane localization of FtsZ-sfGFP. Furthermore, we found that some GVs showed membrane deformations at regions with high accumulation of FtsZ-sfGFP (Figure 3B and S12B, Supporting Information). Deformed regions often had larger curvature than that of GV itself; that is, the regions protruded to the outside. Regional deformations also induced deformation of the whole shape of vesicles into a more ellipsoid-like shape rather than spherical shape. These data indicate that the formation of FtsZ and ZipA complex on membrane provides the direct force for the mechanical deformation of lipid membrane. When the DNA ratio of FtsZ-sfGFP to ZipA was further increased (6 nM FtsZ-sfGFP to 0.75 nM ZipA), however, membrane localization of FtsZ-sfGFP was lost in many GVs and membrane deformation was not observed (Figure S7D, Supporting Information). This suggested that balance between two proteins amount is critical to achieve membrane tethering of FtsZ and produce the deformational force on the membrane. To analyze more quantitatively, we further measured the concentration of coexpressed FtsZ-sfGFP/ZipA in batch reaction with different DNA ratios (Figure S9, Supporting Information). The data suggests that deformation requires high level expression of both FtsZ and ZipA, and especially in the case of FtsZ, it should be over the polymerization threshold, 0.7 μM.

Membrane recruitment was also observed by directly fusing mts to the FtsZ-sfGFP C-terminus, as shown in a previous report[12] (Figure S5F, Supporting Information). However, neither regional deformations nor vesicle shape changes were observed by direct mts fusion. Again, these results support that membrane targeting of FtsZ is not sufficient to induce membrane deformation, but FtsZ-ZipA interaction can exert the force to deform the lipid bilayer.

Since sfGFP fusion seemed to have some influence on FtsZ in aforementioned *in vitro* assays, it is also possible that the observed membrane deformation with coexpression of FtsZ-sfGFP and ZipA is attributed to an artificial effect of sfGFP fusion. To eliminate this possibility, we expressed FtsZ and ZipA without any tag fusions and analyzed membrane deformation by using images of membrane marker Rhod-DOPE (Figure S12A, Supporting Information). Deformation analysis was performed by measuring angle and distance from a center of mass for each point on vesicle membrane. If the vesicle shape is close to a perfect circle, angle-distance plot become flat line because the distance from a center of mass does not change around the circumference. Deformation appears as distorted curves in angle-distance plot because the distance differs from the average radius near a deformed point (Figure S10A, Supporting Information). The graph showed many significant peaks in the case of FtsZ/ZipA coexpression as well as FtsZ-sfGFP/ZipA coexpression (Figure S10B, Supporting Information). It is clear that these deformations are not due to the artifacts during GV formation because such prominent steep peaks were not found in negative controls of sfGFP and ZipA-sfGFP. The frequency of deformed vesicle was calculated based on these analysis (see Methods), and FtsZ/ZipA coexpression showed clear difference from negative controls (Figure S10C, Supporting Information). Thus, we concluded that the membrane deformation was driven by interaction between FtsZ and ZipA, and it was not due to an effect of sfGFP fusion.

To determine whether GTP binding and GTP hydrolysis activity of FtsZ are involved in the ZipA-dependent membrane deformation, we tested FtsZ mutants in combination with ZipA. Here, FtsZ1 (A70T) abolishes GTPase activity but still binds to GTP, whereas FtsZ3 (T108A) loses GTP binding itself.[24] When FtsZ1-sfGFP or FtsZ3-sfGFP was coexpressed with ZipA in POPC 100% GV, clustered regions of sfGFP fluorescence were observed in both cases (Figure 3C, 3D, S12D and S12E, Supporting Information). Thus, neither GTP binding nor hydrolysis reaction appeared to be necessary for FtsZ-ZipA interaction and asymmetric cluster formation. Furthermore, membrane deformations were also observed in both mutants, suggesting that membrane deformation by FtsZ/ZipA can be driven without GTP hydrolysis energy.

In the present study, we demonstrated a cell-free approach to reconstruct the cell division proteins FtsZ, FtsA, and ZipA using the PURE system. The proteins were successfully synthesized and the yield reached the micromolar level in a batch condition. Biochemical analysis confirmed the GTPase activity of FtsZ and the membrane tethering function of FtsA and ZipA. Imaging data visualized bundle-like higher order structures of FtsZ, lipid-to-protein and protein-to-protein interactions, and eventually membrane deformations. Importantly, our cell-free approach enables functional proteins to be obtained while circumventing troublesome protein purification including detergents or a refolding process, as well as artificial Ni-chelating lipids. This simplicity of our strategy would be extremely advantageous compared with the conventional protein purification method, not only for FtsA and ZipA, but also for other proteins with cell toxicity, lethal mutation, or recalcitrance to purification.

The analyses using the *de novo* synthesized proteins provided several new insights into the biochemical property of the Z-ring proteins. First, based on flotation assay and GV imaging, we found that the membrane binding of *E. coli* FtsA depends on anionic lipids (Figure 1C, Figure S3B, Supporting Information, Figure 2D and E). These results are consistent with a study indicating that MinD mts requires anionic lipids to form an amphipathic helix.[27] However, this finding is contrary to a previous study that suggested that FtsA binding to lipid is exerted by hydrophobic interaction and independent of anionic lipid or ionic strength.[5] A possible explanation for these conflicting claims is that the protein refolding process employed in the previous study affected protein structure and biochemical properties. This notion could be supported by the fact that refolded FtsA did not show significant ATP/ADP binding activity,[5] although recent studies indicated that the ATP plays a critical role in FtsA membrane binding[14] and FtsA-

DOI: 10.1021/acssynbio.7b00350
ACS Synth. Biol. XXXX, XXX, XXX−XXX

FtsZ pattern formation.[8] Alternatively, higher salt condition (100−500 mM KCl) used in the previous report[5] could enhance interaction between FtsA and lipid bilayer.

Second, ZipA showed strong affinity to POPC membrane, unless sfGFP was fused at the N-terminus (Figure 1C, Figure 2F, Figure S5D, Supporting Information). These data suggested that, if the N-terminus is free, the N-terminal transmembrane helix can be integrated into the lipid bilayer. Surprisingly, however, the membrane affinity was reduced in the presence of anionic POPG lipid even at the physiological level (20%) (Figure S3D, S5D, Supporting Information). *E. coli* ZipA has an acidic amino acids cluster from Asp(49) to Glu(61), whose 10 amino acids out of 13 are composed of Asp or Glu. Thus, this region may cause a repulsive force against anionic lipids. Previous studies have indicated that *E. coli* cytoplasmic membrane has inhomogeneous lipid patterns and the distribution changes through the cell cycle.[32−34] Therefore, we speculate that opposing effects of anionic lipids on membrane binding of FtsA and ZipA could be a key factor regulating the timing and location of binding partners for FtsZ. Our cell-free approach allows us to reproduce cell division proteins in physiological condition without introducing any mutations or artificial lipid binding motifs and will be a great advantage to reveal fundamental molecular mechanism of cell division.

Finally, imaging data of multiple gene coexpression in GVs also provided new findings in membrane deformation driven by cooperative interaction between FtsZ and ZipA (Figure 3B). Coexpression of ZipA recruited FtsZ-sfGFP to the membrane and induced regional deformations of the lipid membrane. Although GV membrane formed by emulsion transfer method is known to have a trace of residual oil in lipid bilayer[35] and this may influence the mechanical properties of GVs to some extent, image analysis indicated that deformation driven by FtsZ and ZipA was qualitatively different from such artifacts. A similar membrane deformation driven by FtsZ and ZipA was previously reconstructed inside GVs,[9] in which Alexa dye labeled FtsZ was targeted to the membrane by His-tagged ZipA and Ni-NTA lipid. However, there are at least two differences between the present and previous observations. First, our data showed locally accumulated pattern of FtsZ-sfGFP in contrast to the previously found uniform membrane localization of FtsZ. Second, our results of FtsZ mutant suggested that membrane deformation can be induced without GTP hydrolysis reaction (Figure 3C), whereas, in the previous study, membrane deformation was not observed when nonhydrolyzable GTP analog, GMP-PCP, was used. Since ZipA transmembrane helices can form dimers, ZipA can cross-link two of FtsZ filaments.[7] This cross-linking activity of ZipA transmembrane helix cannot be reproduced by Ni-His tag interaction, and cluster formation of FtsZ-ZipA complex observed in the present study is probably attributed to this cross-linking activity because if cross-links happen in various sites FtsZ filaments can assemble into network structure. Furthermore, it has been proposed that cross-linked filaments network could supply contractile force even in the absence of motor proteins or nucleotide hydrolysis.[36] Thus, the presence of native ZipA transmembrane helix can explain why membrane localization pattern and GTP hydrolysis dependency of deformational force were observed differently from the previous result. Indeed, our results are consistent with the recent study, which found that reduction of FtsZ GTPase activity did not significantly change septum constriction rate.[37] However, an alternative possible interpretation for the discrepancy in GTP hydrolysis dependency is that GTPase mutant, used in our study, has slower kinetics of membrane deformation but the difference was not captured in our end point observation.

Although we focused on the three fundamental proteins FtsZ, FtsA, and ZipA, there is abundant room for further progress in combining other subunits or subsystems to obtain a better understanding of the cell division mechanism and also to build a more sophisticated bottom-up self-reproducible system. For instance, the MinCDE system and its Z-ring positioning mechanism, which was recently reconstructed with the FtsZ-ZipA system on supported lipid bilayer,[11] is a good subject to study also in the encapsulated and more elastic lipid environment. Besides, given the finding that FtsZ is released from the septum before cell division is completed,[38] the next important step is to study how downstream divisome proteins assemble into a mature complex and complete cell division. Furthermore, it would be interesting to elucidate how FtsZ polymers accomplish unidirectional treadmilling and recruit the cell wall synthesis complex *in vivo*. Such progress would provide us with insights into how division proteins interact with each other and orchestrate the dynamic cell division reaction.

To the best of our knowledge, this is the first report to show that fundamental cell division proteins were successfully synthesized inside a vesicle compartment and led to membrane deformation. In other words, we established a fundamental biochemical system that can autonomously decode genetic information into functional cytoskeleton proteins, and eventually change the morphology of the compartment. This can lead to the practical construction of a minimal cell that consists of the minimal number of components necessary for cell survival.[39] Although the reconstruction of self-reproduction is one of the great challenges in biology, our approach provides a remarkable advance along with the recent FtsZ reconstruction studies based on purified protein. Since the PURE system, which we used as gene expression machinery in this study, is reconstituted only with individually purified and well-defined factors, it is suitable for the design of a minimal cell. In combination with other previous achievements in cell-free reconstruction, such as lipid metabolism,[40,41] protein transport,[16] energy regeneration,[42] DNA replication,[43] and translation machinery,[20] we believe that our study paves the way to create a self-reproducible minimal cell in a more realistic form and reveal how living cells have gained sophisticated systems.

METHODS

Materials. POPC, POPG, and Rhod-DOPE were purchased from Avanti Polar Lipids. Liquid paraffin, from Wako Pure Chemical Industries, was used for GV preparation. PURE*frex* 2.0 was supplied by GeneFrontier. L-[^{35}S]-Methionine and [γ-^{32}P]-GTP was purchased from PerkinElmer.

DNA Construction. The genes of FtsZ, FtsA, and ZipA were amplified from the genomic DNA of *E. coli* W3110 by PCR and cloned into the pET17b vector. FtsZ-sfGFP was made by fusing sfGFP to the C-terminus of the FtsZ with a linker TCTAGACTCGAG (SRLE). FtsZ-sfGFP-mts is composed of FtsZ ΔC (1−1098 nt), first linker CCCCCTCGACCT-GCAGGCAAGCTT (PPRPAGKL), sfGFP, second linker GGCGGCCGC (GGR), and a membrane targeting sequence (mts) (FIEEEKKGFLKRLFGG) derived from MinD. The N-terminus and C-terminus sfGFP fusions of FtsA and ZipA were constructed by fusing sfGFP with a linker GGATCCACCG-CCACC (GSTAT). On the basis of these plasmid vectors, the

DOI: 10.1021/acssynbio.7b00350
ACS Synth. Biol. XXXX, XXX, XXX−XXX

linear DNA templates for cell-free protein synthesis were amplified by PCR. The linear templates of FtsZ and ZipA were amplified by pET17b-Fw primer (CAGGACCCAACGCTG) and pET17b-Rv primer (GGATATAGTTCCTCCTTTCAGC). The FtsA template was amplified by two-step PCR. In the first PCR, FtsA-opt primer (CTTTAAGAAGGAGATATACCAATGATTAAAGCTACTGATAGAAAACTTGTTG, underline indicates start codon, double underlines indicate optimized nucleotides) was used with the reverse primer pET17b-Rv to reduce the N-terminal GC content of FtsA and increase the expression level. The resulting product was further amplified with PURE universal primer (GAAATTAATACGACTCACTATAGGGAGACCACAACGGTTTCCCTCTAGAAATAATTTTGTTTAACTTTAAGAAGGAGATATACCA) and pET17b-Rv.

***In Vitro* Protein Synthesis.** The cell-free protein synthesis was performed using PURE*frex* 2.0, the latest version of the PURE system. The reaction mixture containing L-[^{35}S]-Methionine was incubated at 37 °C for 3 h. The evaluation of the protein aggregation was performed as previously described.[23] Briefly, some of the sample was separated as the total fraction after the protein synthesis reaction. The rest of the sample was centrifuged at 20 400*g* for 30 min, and the supernatant fraction was collected. Both the total and the supernatant fractions were separated by SDS-PAGE, and the band intensities were quantified by autoradiography. The solubility, an index of protein folding propensity, was defined as the ratio of the supernatant to the total protein, in accordance with a previous study.[23]

GTPase Assay. GTPase activity was measured using radioactive GTP and molybdate. GTP cold/hot-mix was made by mixing 50 mM GTP (cold) and 1.7 μM [γ-^{32}P]-GTP (hot) at 2:1 (v/v) ratio, so that radioactivity was in the range of 50−100 cpm/pmol GTP, and used for GTPase assay. FtsZ or FtsZ-sfGFP was synthesized with the PURE system for 3 h. The PURE system mixture was diluted 5-fold with a buffer including 50 mM HEPES-KOH (pH 7.5), 50 mM KCl, and 10 mM $MgCl_2$ as the final concentration. In this step, RNase A (final 1 ng/μL), DNase I (final 0.04 U/μL), and tetracycline (final 1 μM) were also added to the GTPase reaction mixture in order to reduce background GTPase activity of the PURE system enzymes. GTPase reaction was carried out at 37 °C for 2 h. The reaction was terminated by adding 100 μL of 200 mM H_2SO_4 and 1.5 mM NaH_2SO_4. After termination, 25 μL of 5% (w/v) sodium molybdate and 250 μL of 1-butanol were added. Following 1 min of vortexing, the mixture was separated into the organic solvent layer and the inorganic solvent layer by centrifugation at 9100*g* for 1 min. Chelated ^{32}P was collected from the upper organic layer and the amount was determined by a liquid-scintillation counter.

Preparation of SVs. SVs used in the flotation assay were prepared as follows. Lipids were mixed in chloroform and dried by N_2 gas flow and overnight vacuum. Buffer containing 50 mM HEPES-KOH, 50 mM KCl, and 10 mM $MgCl_2$ was added to dried lipid film to give 20 mg/mL lipid solution. Lipids were then freeze−thawed and sonicated to make SVs. The size of vesicles was confirmed by dynamic light scattering, and those having a peak radius of 50−130 nm were used for the experiments.

Flotation Assay. Flotation assay was performed by following a previously published protocol.[26] PURE system reaction mixture was prepared in a volume of 20 μL supplemented with SVs at a final concentration of 2 mg/mL. After the protein synthesis reaction, 120 μL of 60% sucrose buffer [50 mM HEPES-KOH (pH 7.6), 50 mM KCl, 10 mM $MgCl_2$, 60% (w/v) sucrose] and 100 μL of flotation buffer [50 mM HEPES-KOH (pH 7.6), 50 mM KCl, 10 mM $MgCl_2$] were added to the reaction PURE system mixture, to give 30% sucrose mixture. Twenty microliters of sample was taken from this 30% sucrose mixture as the "Total fraction". Gradient solutions were prepared by layering 200 μL of 30% sucrose mixture, 200 μL of 25% sucrose buffer [50 mM HEPES-KOH (pH 7.6), 50 mM KCl, 10 mM $MgCl_2$, 25% (w/v) sucrose], and 200 μL of flotation buffer from bottom to top in Polycarbonate Centrifuge Tubes (11 × 34 mm, Beckman Coulter). The tubes were ultracentrifuged at 55 000 rpm for 30 min at 25 °C using a TLS-55 rotor (Beckman Coulter). The top 100 μL was taken as "S1". Then, 200 μL was fractionated from the top as the "Liposome fraction". Each fraction was electrophoresed to confirm the protein content

Protein Synthesis Inside GVs and Imaging. The GVs were prepared using the water-in-oil (w/o) emulsion transfer method, as previously described. POPC and/or POPG solubilized in chloroform were mixed with Rhod-DOPE at 0.5 mol % and dried as described in the preparation of SVs to make lipid films. Lipid solutions were prepared by solubilizing lipid films in liquid paraffin at a lipid concentration of 1 mM. Lipid solutions were gently layered on 50 μL of outer solution (1 × PURE*frex* 2.0 buffer solution 1 and 200 mM glucose). In another tube, 10 μL of the PURE*frex* 2.0 reaction mixture supplemented with 200 mM sucrose was added to 50 μL of the lipid oil mixture. This solution was pipetted until it became cloudy and immediately dropped onto the previously prepared liquid paraffin layer. The layered solution was centrifuged at 1600*g* for 5 min at 25 °C. The upper layer was removed and 30 μL of the lower layer containing precipitated GVs was collected. GVs were incubated at 37 °C for 3 h. The samples were imaged using the LSM 5 EXCITER laser scanning microscope (Carl Zeiss) with the Objective Plan-Apochromat 63×/1.4 Oil DIC (Carl Zeiss). A sfGFP and Rhod-DOPE were excited with 488 and 543 nm lasers, respectively. All observations were performed at room temperature.

Image Analysis and Quantification of Membrane Deformation. To analyze the membrane deformation, we analyzed image obtained by confocal microscope using ImageJ to detect the outline of liposome and measure the center of mass. The outlines were detected by using images of membrane marker of Rhod-DOPE. We only analyzed GVs with an area of 1000 pixels or more in order to ensure sufficient spatial resolution. Quantification of deformation using R was performed by taking angle and distance of each point on outlines of vesicle membrane from a center of mass $L(\theta)$ (Supplementary Figure S7). $L(\theta)$ was normalized by average of $L(\theta)$. We counted the GVs as deformed if deformation index D, which was calculated by the following equation, is more than 2.5.

$$D = \sum_{i=0}^{n-1} (L(\theta_{i+1}) - L(\theta_i))^2$$

where n is total number of pixels on outline for each GVs.

■ ASSOCIATED CONTENT

Supporting Information

The Supporting Information is available free of charge on the ACS Publications website at DOI: 10.1021/acssynbio.7b00350.

DOI: 10.1021/acssynbio.7b00350
ACS Synth. Biol. XXXX, XXX, XXX−XXX

Data for solubility assay, FtsZ GTPase assay, Flotation assay, Effect of sucrose and Ficoll 70 on protein synthesis, Single protein expression in GVs, 3D reconstruction of FtsZ bundle image, Multisubunits coexpression in GVs, Line scan analysis of membrane binding, Quantitative analysis of membrane deformation, Supplementary images of GV experiment (Single protein expression), Supplementary images of GV experiment (Multisubunits coexpression) (PDF)

AUTHOR INFORMATION

Corresponding Author

*E-mail: ueda@edu.k.u-tokyo.ac.jp.

ORCID

Takuya Ueda: 0000-0002-7760-8271

Present Address

[‖]Department of Cell Biology, Johns Hopkins University School of Medicine, 855 N. Wolfe Street, Rangos 480, Baltimore, Maryland 21205, United States.

Author Contributions

[§]T.F., F.H., and H.T.M. contributed equally to this work.

Notes

The authors declare no competing financial interest.

ACKNOWLEDGMENTS

We thank Pasquale Stano, Masahiro Takinoue, and Masamune Morita for sharing their GV preparation methods and technical advices, Takashi Kanamori of GeneFrontier Co. (Japan) and Tomoe Murakami for supplying PURE*frex* 2.0, and Bingxin Li for pilot experiments. We also thank Enago (www.enago.jp) for the English language review. This work was supported by JSPS KAKENHI (Grant Numbers 16H06156, 16H00797, 26106003, 16H02089, 26660082, 15H01057, 15K16083) and the Astrobiology Center Project of the National Institutes of Natural Sciences (NINS) (Grant Number 271004, AB281027).

ABBREVIATIONS

GV, giant vesicle; mts, membrane targeting sequence; POPC, 1-palmitoyl-2-oleoyl-*sn*-glycero-3-phosphocholine; POPG, 1-palmitoyl-2-oleoyl-*sn*-glycero-3-phospho-(1′-*rac*-glycerol); Rhod-DOPE, 1,2-dioleoyl-*sn*-glycero-3-phospho-ethanolamine-*N*-lissamine rhodamine B sulfonyl; sfGFP, superfolder green fluorescent protein; SV, small vesicle

REFERENCES

(1) Adams, D. W., and Errington, J. (2009) Bacterial cell division: assembly, maintenance and disassembly of the Z ring. *Nat. Rev. Microbiol. 7*, 642−53.

(2) Haeusser, D., and Margolin, W. (2016) Splitsville: structural and functional insights into the dynamic bacterial Z ring. *Nat. Rev. Microbiol. 14*, 305−319.

(3) Pichoff, S., and Lutkenhaus, J. (2005) Tethering the Z ring to the membrane through a conserved membrane targeting sequence in FtsA. *Mol. Microbiol. 55*, 1722−34.

(4) Hale, C. A., and de Boer, P. A. J. (1997) Direct binding of FtsZ to ZipA, an essential component of the septal ring structure that mediates cell division in E. coli. *Cell 88*, 175−85.

(5) Martos, A., Monterroso, B., Zorrilla, S., Reija, B., Alfonso, C., Mingorance, J., Rivas, G., and Jiménez, M. (2012) Isolation, Characterization and Lipid-Binding Properties of the Recalcitrant FtsA Division Protein from Escherichia coli. *PLoS One 7*, e39829.

(6) Hale, C. A., Rhee, A. C., and Boer, P. A. de. (2000) ZipA-induced bundling of FtsZ polymers mediated by an interaction between C-terminal domains. *J. Bacteriol. 182*, 5153−66.

(7) Skoog, K., and Daley, D. O. (2012) The Escherichia coli cell division protein ZipA forms homodimers prior to association with FtsZ. *Biochemistry 51*, 1407−15.

(8) Loose, M., and Mitchison, T. (2014) The bacterial cell division proteins FtsA and FtsZ self-organize into dynamic cytoskeletal patterns. *Nat. Cell Biol. 16*, 38−46.

(9) Cabré, E. J., Sánchez-Gorostiaga, A., Carrara, P., Ropero, N., Casanova, M., Palacios, P., Stano, P., Jiménez, M., Rivas, G., and Vicente, M. (2013) Bacterial division proteins FtsZ and ZipA induce vesicle shrinkage and cell membrane invagination. *J. Biol. Chem. 288*, 26625−34.

(10) RayChaudhuri, D. (1999) ZipA is a MAP-Tau homolog and is essential for structural integrity of the cytokinetic FtsZ ring during bacterial cell division. *EMBO J. 18*, 2372−83.

(11) Martos, A., Raso, A., Jiménez, M., Petrášek, Z., Rivas, G., and Schwille, P. (2015) FtsZ Polymers Tethered to the Membrane by ZipA Are Susceptible to Spatial Regulation by Min Waves. *Biophys. J. 108*, 2371−2383.

(12) Osawa, M., and Erickson, H. P. (2013) Liposome division by a simple bacterial division machinery. *Proc. Natl. Acad. Sci. U. S. A. 110*, 11000−4.

(13) Szwedziak, P., Wang, Q., Bharat, T., Tsim, M., and Löwe, J. (2014) Architecture of the ring formed by the tubulin homologue FtsZ in bacterial cell division. *eLife 3*, e04601.

(14) Krupka, M., Cabré, E. J., Jiménez, M., Rivas, G., Rico, A. I., and Vicente, M. (2014) Role of the FtsA C terminus as a switch for polymerization and membrane association. *mBio 5*, e02221.

(15) Moritani, Y., Nomura, S. M., Morita, I., and Akiyoshi, K. (2010) Direct integration of cell-free-synthesized connexin-43 into liposomes and hemichannel formation. *FEBS J. 277*, 3343−52.

(16) Matsubayashi, H., Kuruma, Y., and Ueda, T. (2014) In vitro synthesis of the *E. coli* Sec translocon from DNA. *Angew. Chem., Int. Ed. 53*, 7535−8.

(17) Noireaux, V., and Libchaber, A. (2004) A vesicle bioreactor as a step toward an artificial cell assembly. *Proc. Natl. Acad. Sci. U. S. A. 101*, 17669−74.

(18) Ota, S., Yoshizawa, S., and Takeuchi, S. (2009) Microfluidic Formation of Monodisperse, Cell-Sized, and Unilamellar Vesicles. *Angew. Chem., Int. Ed. 48*, 6533−6537.

(19) Fujii, S., Matsuura, T., Sunami, T., Nishikawa, T., Kazuta, Y., and Yomo, T. (2014) Liposome display for in vitro selection and evolution of membrane proteins. *Nat. Protoc. 9*, 1578−91.

(20) Caschera, F., Lee, J., Ho, K., Liu, A., and Jewett, M. (2016) Cell-free compartmentalized protein synthesis inside double emulsion templated liposomes with in vitro synthesized and assembled ribosomes. *Chem. Commun. 52*, 5467−9.

(21) Shimizu, Y., Inoue, A., Tomari, Y., Suzuki, T., Yokogawa, T., Nishikawa, K., and Ueda, T. (2001) Cell-free translation reconstituted with purified components. *Nat. Biotechnol. 19*, 751−5.

(22) Chen, Y., and Erickson, H. P. (2005) Rapid in vitro assembly dynamics and subunit turnover of FtsZ demonstrated by fluorescence resonance energy transfer. *J. Biol. Chem. 280*, 22549−54.

(23) Niwa, T., Ying, B. -W. W., Saito, K., Jin, W., Takada, S., Ueda, T., and Taguchi, H. (2009) Bimodal protein solubility distribution revealed by an aggregation analysis of the entire ensemble of Escherichia coli proteins. *Proc. Natl. Acad. Sci. U. S. A. 106*, 4201−6.

(24) Dai, K., Mukherjee, A., Xu, Y., and Lutkenhaus (1994) Mutations in ftsZ that confer resistance to SulA affect the interaction of FtsZ with GTP. *J. Bacteriol. 176*, 130−136.

(25) Ma, X., Ehrhardt, D., and Margolin, W. (1996) Colocalization of cell division proteins FtsZ and FtsA to cytoskeletal structures in living Escherichia coli cells by using green fluorescent protein. *Proc. Natl. Acad. Sci. U. S. A. 93*, 12998−13003.

(26) Pykäläinen, A., Boczkowska, M., Zhao, H., Saarikangas, J., Rebowski, G., Jansen, M., Hakanen, J., Koskela, E., Peränen, J., Vihinen, H., Jokitalo, E., Salminen, M., Ikonen, E., Dominguez, R., and

DOI: 10.1021/acssynbio.7b00350
ACS Synth. Biol. XXXX, XXX, XXX−XXX

Lappalainen, P. (2011) Pinkbar is an epithelial-specific BAR domain protein that generates planar membrane structures. *Nat. Struct. Mol. Biol. 18*, 902−907.
(27) Szeto, T., Rowland, S., Habrukowich, C., and King, G. (2003) The MinD membrane targeting sequence is a transplantable lipid-binding helix. *J. Biol. Chem. 278*, 40050−6.
(28) Osawa, M., Anderson, D. E., and Erickson, H. P. (2009) Curved FtsZ protofilaments generate bending forces on liposome membranes. *EMBO J. 28*, 3476−84.
(29) Soga, H., Fujii, S., Yomo, T., Kato, Y., Watanabe, H., and Matsuura, T. (2014) In Vitro Membrane Protein Synthesis Inside Cell-Sized Vesicles Reveals the Dependence of Membrane Protein Integration on Vesicle Volume. *ACS Synth. Biol. 3*, 372−379.
(30) Gonzalez, J., Velez, M., Andreu, J. M., Vicente, M., and Rivas, G. (2003) Essential Cell Division Protein FtsZ Assembles into One Monomer-thick Ribbons under Conditions Resembling the Crowded Intracellular Environment. *J. Biol. Chem. 278*, 37664−37671.
(31) Groen, J., Foschepoth, D., Brinke, E., te Boersma, A., Imamura, H., Rivas, G., Heus, H., and Huck, W. (2015) Associative Interactions in Crowded Solutions of Biopolymers Counteract Depletion Effects. *J. Am. Chem. Soc. 137*, 13041−8.
(32) Fishov, and Woldringh (1999) Visualization of membrane domains in Escherichia coli. *Mol. Microbiol. 32*, 1166−72.
(33) Oliver, P. M., Crooks, J. A., Leidl, M., and Yoon, E. J. (2014) Localization of anionic phospholipids in Escherichia coli cells. *J. Bacteriol. 196*, 3386−98.
(34) Revelo, N. H., Kamin, D., Truckenbrodt, S., Wong, A. B., Reuter-Jessen, K., Reisinger, E., Moser, T., and Rizzoli, S. O. (2014) A new probe for super-resolution imaging of membranes elucidates trafficking pathways. *J. Cell Biol. 205*, 591−606.
(35) Kamiya, K., Kawano, R., Osaki, T., Akiyoshi, K., and Takeuchi, S. (2016) Cell-sized asymmetric lipid vesicles facilitate the investigation of asymmetric membranes. *Nat. Chem. 8*, 881−889.
(36) Sun, S., Walcott, S., and Wolgemuth, C. (2010) Cytoskeletal Cross-linking and Bundling in Motor-Independent Contraction. *Curr. Biol. 20*, R649−R654.
(37) Coltharp, C., Buss, J., Plumer, T., and Xiao, J. (2016) Defining the rate-limiting processes of bacterial cytokinesis. *Proc. Natl. Acad. Sci. U. S. A. 113*, E1044−E1053.
(38) Söderström, B., Skoog, K., Blom, H., Weiss, D. S., von Heijne, G., and Daley, D. O. (2014) Disassembly of the divisome in Escherichia coli: evidence that FtsZ dissociates before compartmentalization. *Mol. Microbiol. 92*, 1−9.
(39) Luisi, P., Ferri, F., and Stano, P. (2006) Approaches to semi-synthetic minimal cells: a review. *Naturwissenschaften 93*, 113.
(40) Kuruma, Y., Stano, P., Ueda, T., and Luisi, P. L. (2009) A synthetic biology approach to the construction of membrane proteins in semi-synthetic minimal cells. *Biochim. Biophys. Acta, Biomembr. 1788*, 567−74.
(41) Scott, A., Noga, M., Graaf, P., de Westerlaken, I., Yildirim, E., and Danelon, C. (2016) Cell-Free Phospholipid Biosynthesis by Gene-Encoded Enzymes Reconstituted in Liposomes. *PLoS One 11*, e0163058.
(42) Kuruma, Y., and Ueda, T. (2015) The PURE system for the cell-free synthesis of membrane proteins. *Nat. Protoc. 10*, 1328−44.
(43) Fujiwara, K., Katayama, T., and Nomura, S. M. (2013) Cooperative working of bacterial chromosome replication proteins generated by a reconstituted protein expression system. *Nucleic Acids Res. 41*, 7176−83.

DOI: 10.1021/acssynbio.7b00350
ACS Synth. Biol. XXXX, XXX, XXX−XXX